Transient requirement for ganglion cells during assembly of retinal synaptic layers

Jeremy N. Kay[1,*], Tobias Roeser[1,*], Jeff S. Mumm[2,*], Leanne Godinho[2,*], Ana Mrejeru[1], Rachel O. L. Wong[2] and Herwig Baier[1,†]

[1]Program in Neuroscience and Department of Physiology, University of California, San Francisco, 513 Parnassus Avenue Box 0444, San Francisco, CA 94143, USA
[2]Department of Anatomy and Neurobiology, Washington University School of Medicine, 660 South Euclid, St Louis, MO 63110, USA
*These authors contributed equally to this work
†Author for correspondence (e-mail: hbaier@itsa.ucsf.edu)

Accepted 28 November 2003

Development 131, 1331-1342
Published by The Company of Biologists 2004
doi:10.1242/dev.01040

Summary

The inner plexiform layer (IPL) of the vertebrate retina comprises functionally specialized sublaminae, representing connections between bipolar, amacrine and ganglion cells with distinct visual functions. Developmental mechanisms that target neurites to the correct synaptic sublaminae are largely unknown. Using transgenic zebrafish expressing GFP in subsets of amacrine cells, we imaged IPL formation and sublamination in vivo and asked whether the major postsynaptic cells in this circuit, the ganglion cells, organize the presynaptic inputs. We found that in the *lak/ath5* mutant retina, where ganglion cells are never born, formation of the IPL is delayed, with initial neurite outgrowth ectopically located and grossly disorganized. Over time, the majority of early neurite projection errors are corrected, and major ON and OFF sublaminae do form. However, focal regions of disarray persist where sublaminae do not form properly. Bipolar axons, which arrive later, are targeted correctly, except at places where amacrine stratification is disrupted. The *lak* mutant phenotype reveals that ganglion cells have a transient role organizing the earliest amacrine projections to the IPL. However, it also suggests that amacrine cells interact with each other during IPL formation; these interactions alone appear sufficient to form the IPL. Furthermore, our results suggest that amacrines may guide IPL sublamination by providing stratification cues for other cell types.

Movies and supplemental data available online

Key words: Retina, Neural differentiation, Axon guidance, Target selection, Zebrafish

Introduction

Neural circuits with specific functions are frequently organized into laminae or columns within the vertebrate central nervous system (Sanes and Yamagata, 1999; Wong and Lichtman, 2002). For example, in the visual system, projections from the two eyes are segregated into eye-specific laminae in the dorsal lateral geniculate nucleus and into ocular dominance columns in the visual cortex. A layered arrangement of synaptic connections is also found in the tectum of birds and fish and in the dorsal spinal cord and hippocampus of mammals (Sanes and Yamagata, 1999). The relative importance of neural activity in establishing laminar and columnar patterns of synaptic connectivity during development is still debated (Constantine-Paton et al., 1990; Katz and Shatz, 1996; Katz and Crowley, 2002; Zhang and Poo, 2001). However, pre- and postsynaptic cell-cell interactions before and during synapse formation are widely thought to play an important role in this process (Wong and Lichtman, 2002).

The highly laminated structure of the retina makes it an ideal model system for studying the mechanisms of synaptic layer formation. In the mature inner plexiform layer (IPL; Fig. 1A), connections between retinal ganglion cells (GCs) and their presynaptic partners, the amacrine cells (ACs) and bipolar cells (BCs), are broadly segregated into ON or OFF sublayers, each representing circuits that are either depolarized (ON) or hyperpolarized (OFF) by increased illumination (Famiglietti and Kolb, 1976). The ON and OFF sublayers are further divided into functionally specialized sublaminae (e.g. Roska and Werblin, 2001; Wässle and Boycott, 1991). The IPL and its sublaminae extend continuously across the retina, a feature that is important for lateral processing of visual information. Elucidating the mechanisms underpinning IPL formation and sublamination will provide important insights into how neural circuits become precisely wired during development.

GCs are the earliest cell type to differentiate in the vertebrate retina, followed closely by ACs with whom they form the first synaptic circuits (reviewed by Livesey and Cepko, 2001) [also shown in zebrafish (Hu and Easter, 1999; Schmitt and Dowling, 1999)]. Later, BCs differentiate and synapse onto GCs and ACs, conveying photoreceptor signals to the inner retina. Although it is evident that the developing dendrites of GCs undergo a structural refinement that gradually restricts them to specific IPL sublaminae (Maslim and Stone, 1988; Bodnarenko and Chalupa, 1993; Bodnarenko et al., 1995), it is

not known whether the neurites of ACs grow directly into a specific IPL layer or whether structural rearrangements are part of the process by which AC arbors find their appropriate laminae. Furthermore, it is unclear whether AC and BC axonal terminals are sculpted on a scaffold initially laid down by GC dendrites or are otherwise dependent on GC-derived cues. Günhan-Agar et al. (Günhan-Agar et al., 2000) and Williams et al. (Williams et al., 2001) showed that, in rats and ferrets, ACs and BCs develop and maintain ON and OFF stratification patterns after experimentally induced degeneration of GCs. Although elegant in design, these experiments do not unequivocally rule out a role for GCs in IPL organization, because GCs were present and had differentiated prior to ablation. Furthermore, some ACs are already stratified at birth in rodents (Reese et al., 2001; Stacy and Wong, 2003), prior to the manipulations that eliminated GCs.

We thus investigated the role of GCs in organizing lamination of the IPL using a zebrafish mutant in which GCs are never present. The *lakritz* (*lak*) gene encodes Atonal homologue 5 (Ath5), a basic-helix-loop-helix-transcription

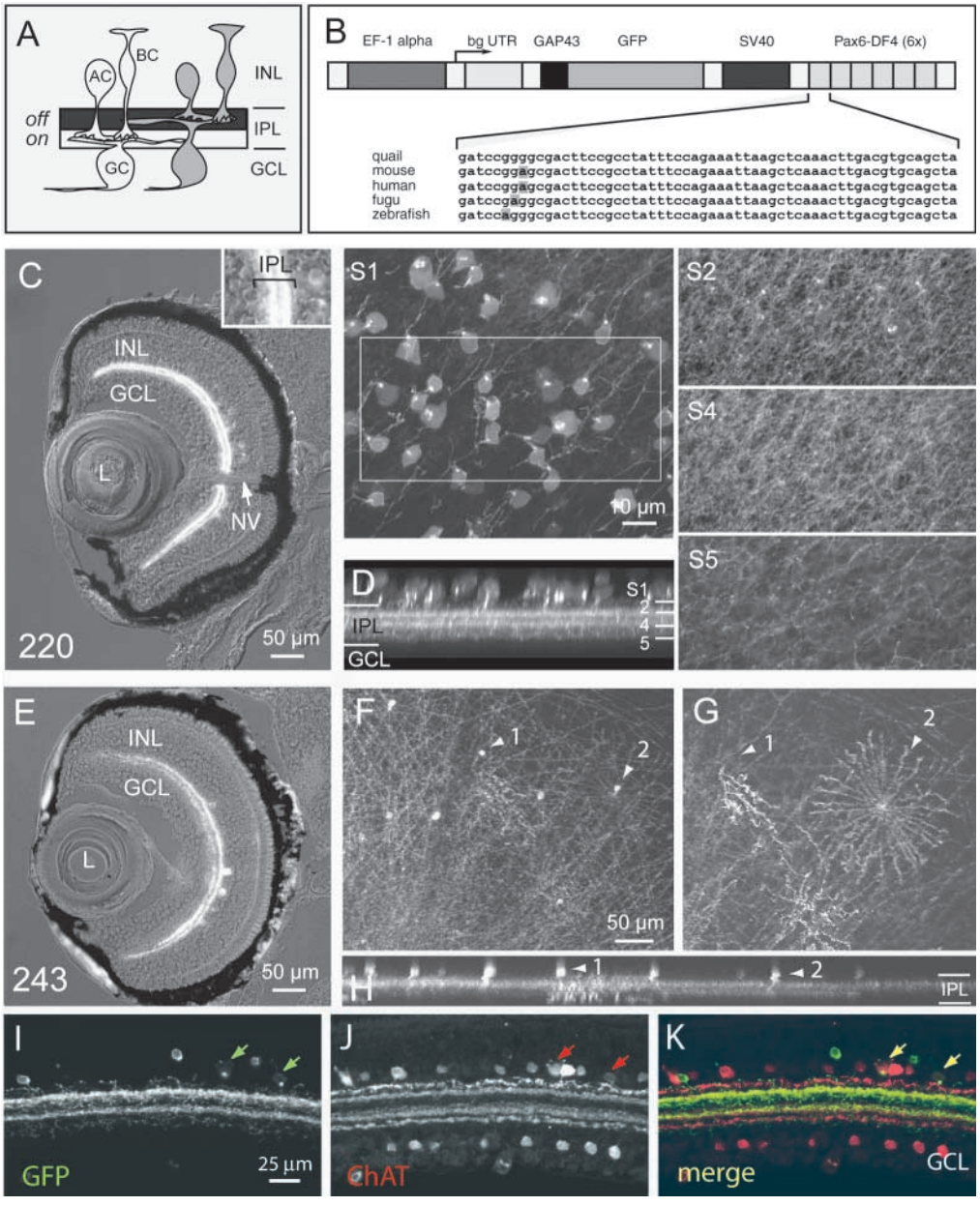

Fig. 1. Subpopulations of ACs express GFP in *Pax6-DF4:mGFP* transgenic zebrafish lines. (A) Schematic of inner retinal organization in mature vertebrates. Connections between ganglion cells (GCs), amacrine cells (ACs) and bipolar cells (BCs) are localized to the inner plexiform layer (IPL). The IPL is further organized into ON and OFF sublaminae that occupy approximately the inner and outer halves of the IPL, respectively. (B) The construct used to derive *Pax6-DF4:mGFP* transgenic lines. Expression of the Gap-43GFP fusion protein was driven by a hexamer of the 58 bp *pax6* DF4 element, located downstream of the SV40 poly-A sequence, and by an upstream *EF1α* promoter. The sequence of the highly conserved DF4 element is shown. (C) Cross-sectional view of GFP$^+$ ACs and their neurites in the IPL of line 220 7 dpf retina. GFP fluorescence is superimposed on a Nomarski image of a section through the eye. Two bright sublaminae are evident in the IPL (see higher magnification image, inset). (D) Digital rotation of a confocal image stack, providing an orthogonal view of a region of inner retina of a line 220 retinal wholemount at 9 dpf. S1 is an optical slice of this field of view showing sparsely distributed GFP$^+$ neurites close to the AC cell bodies. S2-5 are image planes within the boxed region in S1. The two major GFP$^+$ sublaminae are S2 and S4; note also sparse innervation of sublaminae S1 and S5 by GFP$^+$ neurites. (E) Cross-sectional view of the eye of an 7 dpf line 243 fish. (F) Morphology of individual GFP$^+$ cells in line 243. Maximum projection of a confocal image stack (47 µm total) through the inner retina of a retinal whole mount at 35 dpf. (G) Arbors of a few isolated ACs (1, 2 in F) at an IPL depth closer to the GCL. (H) Digital rotation of the complete image stack providing orthogonal views of cells 1 and 2. Cell 1 has a diffuse asymmetric arbor spanning the thickness of the IPL. By contrast, cell 2 has a radially symmetric arbor stratifying in the ON sublamina. (I-K) Cross-sections of adult line 220 retina immunolabeled for ChAT. The two bright GFP$^+$ laminae in line 220 coincide with the two major ChAT-immunopositive bands in sublaminae S2 and S4. Some, but not all, GFP$^+$ cells are also immunoreactive for ChAT (arrows). GCL, ganglion cell layer; INL, inner nuclear layer; IPL, inner plexiform layer; NV, optic nerve; dpf, days post-fertilization; L, lens.

factor required specifically for the genesis of GCs (Kay et al., 2001; Brown et al., 2001; Wang et al., 2001). In *lak* mutants, the first wave of retinal neurogenesis, in which GCs are normally made, fails to occur. As a result, progenitors are prevented from adopting the GC fate (Kay et al., 2001). However, ACs and all other cell types differentiate on time, and an IPL is present (Kay et al., 2001). The specificity of this genetic lesion allowed us to analyze the behavior of ACs in the absence of GCs. For this purpose, we generated transgenic zebrafish in which stable subpopulations of ACs express green fluorescent protein (GFP). GFP expression in these lines marks ACs earlier in their development than most other known markers (Pow et al., 1994), allowing us to visualize the dynamic behavior of GFP-labeled AC neurites in vivo from the earliest stages of neurite outgrowth. Because the zebrafish retina develops rapidly, we were able to continuously monitor IPL development from its formation until segregation into ON and OFF sublaminae, providing the first in vivo view of how functionally distinct synaptic layers arise in a CNS structure during development. Our observations reveal that whereas elimination of GCs causes specific temporal and spatial perturbations in IPL formation, amacrine cells can assume a central role in the formation of synaptic laminae in the retina.

Materials and methods

Generation of *Pax6-DF4:mGFP* transgenic lines

We used a membrane-targeted version of GFP to generate reporter lines that label subsets of ACs. GFP5 (Siemering et al., 1996) was fused at its N terminal to the first 20 amino acids of zebrafish Gap43. This sequence is palmitoylated at the cysteines in positions 3 and 4 and targets the protein to the membrane (Skene and Virag, 1989; Zuber et al., 1989). The DF4 sequence is a 58 bp enhancer element, isolated from the EP enhancer located within the first intron of the *pax6* locus (Plaza et al., 1995; Kammandel et al., 1999). We found that quail DF4 (kindly provided by S. Saule), when combined with a truncated *EF1α* promoter, derived from the pESG vector (kindly provided by C.B. Chien and D. Gilmour) (Johnson and Krieg, 1994), or with the endogenous zebrafish *pax6* promoter (P0) (Plaza et al., 1995), drives transgene expression in ACs and, in some lines, weakly in GCs (T.R. and H.B., unpublished). The GFP^+ AC subpopulation is stable for more than five generations within one line.

The linearized plasmid (Fig. 1B) was injected into zebrafish embryos at the one-cell stage, following standard procedures (Stuart et al., 1988; Higashijima et al., 1997). The injected embryos were selected for transient GFP expression one day later and raised to adulthood. We recovered nine founders from 70 injected fish (13%), a rate within the range of those previously reported for this technology. Founder fish were crossed to non-transgenic fish, and GFP-expressing progeny were raised to generate a stable line. To visualize IPL formation, the experiments in this study were carried out on three lines: *Pax6-DF4:mGFP*^{s220}, *Pax6-DF4:mGFP*^{s243}, and *Pax6-DF4:mGFP*^{s244}. We will refer to these lines as 220, 243 and 244 throughout this paper. We also generated several lines with a similar construct, which was lacking the membrane-targeting signal, but was otherwise identical to the one shown in Fig. 1B. Six of 26 injected fish (23%) transmitted the transgene to the next generation.

Identification of *lak* mutants

Homozygous *lak* mutant embryos (*lak*$^{th241/th241}$) (Kelsh et al., 1996) were identified at 2 days post-fertilization (dpf) in live imaging experiments by the abnormal laminar position of GFP^+ ACs. This method was validated by RFLP genotyping for the *lak*^{th241} allele (Kay et al., 2001). Older larvae were scored as *lak* mutants based on their visual background adaptation defect, which results in dark pigmentation (Kelsh et al., 1996), or, for some experiments, by immunostaining for GCs (Kay et al., 2001).

Immunocytochemistry

ChAT

Adult 220 transgenic fish were euthanized using Tricaine (0.02% w/v in 0.3×Danieau's solution). Following decapitation, their eyes were removed and retinas dissected out and fixed in 4% paraformaldehyde (PFA) in 0.1 M phosphate-buffered saline (PBS), pH 7.4, for 2.5 hours. Vibratome sections (50 μm) were cut and incubated in anti-ChAT (AB144P, Chemicon) diluted 1:100 in PBS containing 5% normal donkey serum (NDS) and 0.5% Triton X-100, for 36 hours with gentle agitation. After several rinses in PBS, sections were blocked with 5% NDS in PBS for 1 hour and then incubated in secondary antibody, Alexa 568 donkey anti-goat (Molecular Probes) at 1:1000 in 5% NDS in PBS for 2.5 hours with gentle agitation. After several rinses in PBS, sections were cover-slipped in Gelmount.

PKC

The progeny of a 220/+; *lak*$^{th241/+}$ incross were fixed in 4% PFA/PBS at 5 dpf, cryosectioned (12 μm), and immunostained for PKC as described (Kay et al., 2001). Single confocal scans were used to detect PKC immunofluorescence and native GFP fluorescence simultaneously.

GFP

Whole-mount embryos or cryosections were stained as described (Kay et al., 2001) using rabbit anti-GFP (Molecular Probes A-11122; 1:4000 dilution). To permeabilize 3.5 dpf embryos, they were incubated with 0.1% collagenase in PBS for 90 minutes prior to antibody staining.

Live imaging

Embryos/larvae were maintained in embryo medium (0.3×Danieau's solution with 100 units/ml penicillin and 100 μg/ml streptomycin) at 28.5°C prior to imaging. At 15 hours post-fertilization (hpf), 1-phenyl-2-thiourea (PTU) was added to embryo medium at a final concentration of 0.003% (w/v) in order to block pigmentation in the eye. Prior to imaging, chorions were manually removed and the larvae transferred to a solution of embryo medium containing 0.003% PTU and 0.02% (w/v) Tricaine. Larvae were then embedded in a petri dish (Falcon # 35-3037) in 0.5% low melting point agarose dissolved in embryo medium containing PTU and Tricaine. Dishes were placed in a temperature controlled stage (Cell Microtemp Systems) and recordings were performed at 28-30°C. Typically up to ten fish were aligned in series to enable imaging several fish during each recording session. Images were acquired and presented primarily from the peripheral retina because the lens distorted images of the central-most part of the retina.

Confocal image stacks were acquired using either the BioRad 1024M or Olympus FV500. Long working distance water objectives, including 20× Nikon (NA 0.5), 40× (NA 0.8) and 60× (NA 0.9) Olympus objectives, were used. To reconstruct cells and their processes, a series of optical planes were collected in the *z* dimension (*z*-stack), and collapsed into a single image (maximum intensity or *z*-projection) or rendered in three dimensions to provide views of the image stack at different angles. The step size for each *z*-stack was chosen upon calculation of the theoretical *z*-resolution of the objective used (typically 0.5-1.0 μm). Time-lapse imaging was carried out by collecting *z*-stacks encompassing the same cells within a selected region per retina at various intervals (typically once every hour or more, and for total recording periods up to around 40 hours). Image analysis was performed offline, using Metamorph (Universal Imaging) to generate image alignments, orthogonal rotations and movies of the *z*-stacks.

Generation and analysis of chimeras

Chimeric embryos were generated by standard methods (Ho and Kane, 1990). The progeny of a 220/220; *lak*$^{th241/+}$ incross were used as donors, and non-transgenic *lak*$^{th241/+}$ incross progeny were used as hosts. At the 1000-cell stage, 10-50 cells were removed from a donor and transplanted to the animal pole of the host blastula. Donors were genotyped by RFLP (Kay et al., 2001). Chimeras were treated with PTU, fixed at 3.5 dpf (after AC sublamination) and immunostained in whole mount with anti-GFP. Individual ACs were imaged on a confocal microscope (BioRad 1024) and reconstructed (see above). For some experiments, chimeras were allowed to survive until 7 dpf, and then sectioned and immunostained with anti-GFP. Only sections taken through the center of the retina (as determined by maximal lens diameter) were used to score sublamination of GFP$^+$ AC neurites, thereby preventing section angle from confounding the analysis. Images were collected using single confocal scans.

Results

The DF4 element of the *Pax6* enhancer drives GFP expression in a diverse subset of ACs

We microinjected a DNA construct encoding membrane-targeted GFP (mGFP) under control of the retina-specific DF4 element of the *pax6* genomic locus to generate stable transgenic lines. The endogenous DF4 element is 58 bp and is located in the first intron of the *pax6* gene. Its location is conserved in all vertebrates studied so far, and its sequence is at least 98% identical between human, mouse, quail, fugu and zebrafish (Fig. 1B) (Kammandel et al., 1999; Miles et al., 1998; Plaza et al., 1995). We used the quail DF4 sequence (Plaza et al., 1995), which is identical to the zebrafish sequence except for a single G to A transition at the sixth position (Fig. 1B). Three reporter lines (named 220, 243, and 244) were generated, which express mGFP in small subpopulations of ACs (see supplemental data S1 at http://dev.biologists.org/supplemental for more details about GFP expression in these lines). The GFP$^+$ cells are ACs based on soma position in the inner nuclear layer (INL), markers and single-cell morphology. In all lines, GFP$^+$ AC neurites innervate two major IPL sublaminae (Fig. 1C-K). The GFP$^+$ sublaminae co-labeled for choline acetyltransferase (ChAT) immunoreactivity, which marks the cholinergic ACs and the well-characterized pattern of IPL innervation by their neurites. This double-labeling demonstrates that the major GFP$^+$ bands correspond to sublamina 2 (an OFF layer) and sublamina 4 (an ON layer; Fig. 1I-K) (Yazulla and Studholme, 2001). Only some of the GFP$^+$ somata are also ChAT-immunoreactive (IR), indicating that the two markers do not label the same AC population, but rather separate populations that share common sublaminar targets. The neurite lamination patterns of GFP$^+$ ACs in the juvenile and adult retina (Fig. 1) resemble those observed in embryonic and larval animals (see below). We conclude that *Pax6-DF4*-driven GFP expression is stable in a subpopulation of ACs through adulthood.

The Pax6 homeodomain transcription factor is expressed in all retinal neuroblasts (Marquardt et al., 2001), a feature that is recapitulated in our lines (Fig. 2A). Later in development, endogenous Pax6 becomes restricted to a subset of ACs in goldfish (Hitchcock et al., 1996), zebrafish (Masai et al., 2003) and mouse (Marquardt et al., 2001). A similar restriction of DF4-driven GFP to ACs is also observed in our lines. However, Pax6-immunoreactive ACs are much more numerous than the GFP$^+$ ACs (Masai et al., 2003). Thus, our reporter lines, although providing a useful in vivo marker for ACs, do not fully reproduce the endogenous Pax6 expression pattern.

The *Pax6-DF4:mGFP* lines permit in vivo imaging of IPL formation and sublamination

Using confocal microscopy, we imaged the eyes of living transgenic zebrafish maintained in a temperature-controlled chamber over several hours to days. In all the transgenic lines, GFP expression is observed in neuroblasts on the first day post-fertilization (dpf), prior to the onset of retinal neurogenesis at 30 hours post-fertilization (hpf; Fig. 2A). As neurogenesis progresses, GFP expression in neuroblasts is diminished and becomes more apparent in ACs. GFP-expressing AC neurites begin to form a plexus parallel to, and approximately two or three cell bodies away from, the internal limiting membrane (ILM) at the beginning of the third dpf (Fig. 2A; 54 hpf). This plexus corresponds to the nascent IPL, as it appears in the expected location and around the time that AC processes first enter the IPL (Schmitt and Dowling, 1999).

Time-lapse imaging revealed that GFP$^+$ AC neurites are progressively added to the forming IPL in a 'clockface' progression (Fig. 2B; see Movie 1 at http://dev.biologists.org/supplemental). The nascent IPL recruits neurites from adjacent regions in order to propagate laterally. The progression of IPL innervation trails the anterior-to-posterior wave of AC neurogenesis (Hu and Easter, 1999) by ~10 hours. The GFP$^+$ plexus is initially unstratified; sublamination of GFP-labeled neurites starts in the developmentally more advanced (nasoventral) part of the retina at around 65 hpf and spreads dorsally, again in a clockface progression (Fig. 2C; see Movie 2 at http://dev.biologists.org/supplemental). Sublamination commences at approximately 20 hours after an IPL first becomes visible and is complete throughout the retina by about 90 hpf, an age that roughly coincides with onset of behavioral responses to moving stimuli (Easter and Nicola, 1996).

IPL formation is delayed in *lak* mutants

We next used *lak* mutants to ask how the IPL develops in the absence of GCs, the major postsynaptic target of the ACs (Fig. 3; see Movies 3A,B). Our time-lapse recordings revealed that the earliest steps of IPL formation were severely affected in *lak* mutants. First, we observed a marked delay in the formation of the IPL. As illustrated in Fig. 3, an IPL is present in the wild-type inner retina at 50 hpf but it is not apparent until 55-57 hpf in the *lak* retinas. Quantitative analysis confirms this observation: Of 45 siblings concurrently imaged from 48 to 85 hpf, an IPL had appeared in 89% of wild-type retinas (32 of 36) at the earliest time point (48-52 hpf). By contrast, only 11% (1/9) of *lak* mutants in this clutch had developed an IPL by 54 hpf. In a separate experiment, we sorted embryos according to the presence or absence of an IPL at 48-50 hpf. Although 97% of wild-type siblings (33/34) possessed an IPL at this age, only 22% (2/9) of mutants had an IPL, thus supporting our conclusion that IPL appearance is delayed in the absence of GCs. Nevertheless, all *lak* mutants eventually did develop an IPL, indicating that GCs are not essential for its formation.

Morphogenesis of the early IPL is disrupted in *lak* mutants

Our time-lapse recordings also showed that, when the IPL first

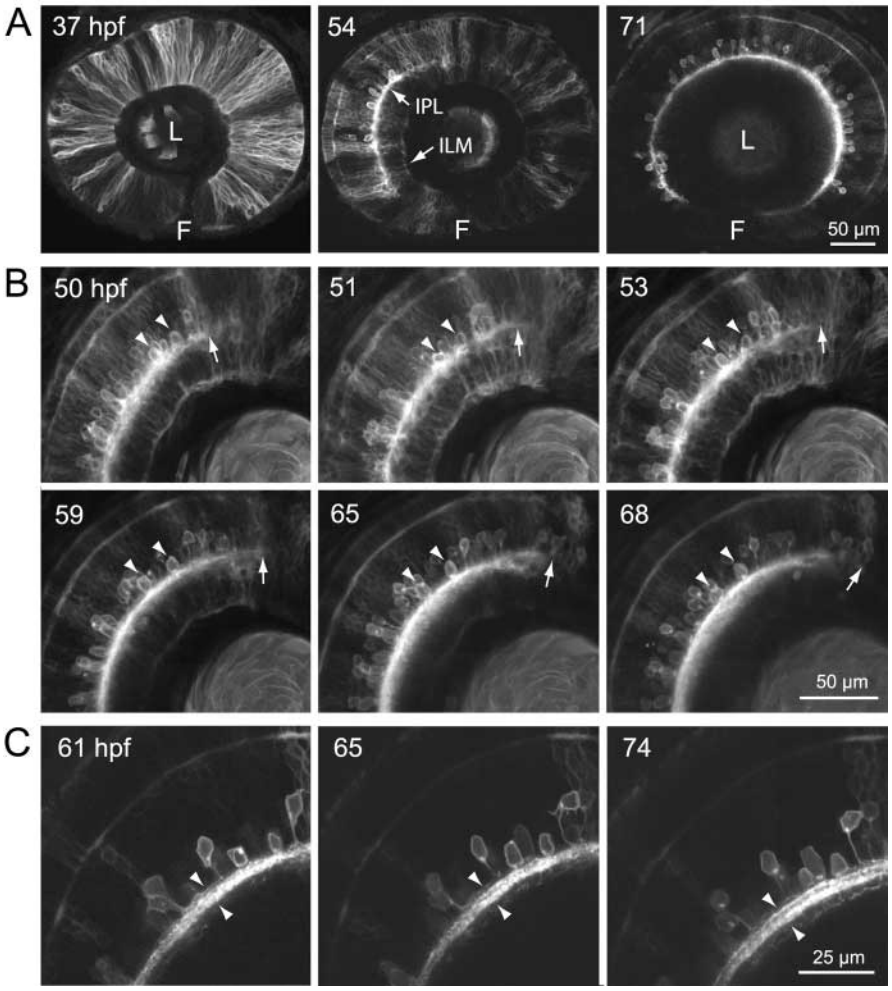

Fig. 2. In vivo visualization of IPL formation and sublamination in *Pax6-DF4:mGFP* line 220. (A) GFP expression at different stages of development in line 220. At 37 hpf, expression is present in neuroblasts with processes spanning the thickness of the retina. By 54 hpf, GFP expression becomes gradually confined to ACs whose neurites take part in forming a continuous inner plexiform layer (IPL), located approximately four or five cell bodies away from the internal limiting membrane (ILM). GFP expression becomes almost exclusively confined to ACs and their neurites by 71 hpf. Note that anterior retina (left) develops before posterior. L, lens; F, choroid fissure (marks ventral retina). (B) Time-lapse confocal images showing progressive addition of GFP^+ ACs over time. Each image is a *z*-projection of a 19 μm confocal image stack. Arrowheads indicate the same cells in all time frames. Arrow marks the approximate locations of emerging GFP-expression in ACs and neurites that contribute to the forming IPL. (C) Appearance of sublamination in the IPL. Each image is a *z*-projection of a 3 μm stack of confocal planes. Arrowheads indicate the same region across time points. For (B,C), dorsal retina is towards the right. Time-lapse movies of B and C (Movies 1 and 2) can be found at http://dev.biologists.org/supplemental).

forms in *lak* mutants, its organization is abnormal. GFP^+ AC neurites initially elaborate to form an early plexus at, or very close to, the ILM in *lak* mutants (Fig. 3). This contrasts with the wild-type retina, in which a laterally organized IPL forms several cell bodies away (some 25 μm) from the ILM (Fig. 2A, Fig. 3). The ectopic location and disrupted appearance of the early IPL, more clearly evident at higher magnification (Fig. 4A), was seen in all *lak* mutants we imaged (n>30 animals). Time-lapse imaging revealed initial AC projection errors in *lak* mutants to be transient – the nascent IPL translocates outward to assume a more typical position with time (Fig. 4A,B, see Movie 3B at http://dev.biologists.org/supplemental).

As morphogenesis of the IPL continues (between 60-70 hpf), *lak* mutants begin to show a variable phenotype. Although some stretches of mutant IPL look relatively normal, forming a smooth plexus in the correct orientation parallel to the ILM (Fig. 4E, arrow 1), other patches show several different types of disorganization that are never seen in age-matched wild-type retinas (see Movies 4A-D at http://dev.biologists.org/supplemental). Four main categories of disorganization were seen: (1) gaps in the GFP^+ plexus (Fig. 4E, arrow 2); (2) parts of the GFP^+ plexus oriented perpendicular or obliquely to the ILM (Fig. 4E, arrow 3); (3) non-laminar agglomerations of GFP^+ cell bodies (Fig. 4E, arrow 4) or neurites (Fig. 4C-D,F-G); and (4) AC neurites growing parallel or oblique to the ILM before either joining the IPL (Fig. 4E), or joining with other AC processes outside the IPL (Fig. 4D,F-G). In every mutant retina examined (n>30), the IPL showed all four types of disorganization, although the number of errors, and their degree of severity, was variable. Errors did not seem specific to any one region of the retina. Time-lapse imaging showed that most of these errors were transient: IPL disorganization was most severe at early stages of IPL formation and improved over time (Fig. 3; Fig. 4A,B; see Movie 3B at http://dev.biologists.org/supplemental). Although errors that resemble those of the nascent IPL persist in the mature retina (see below), ACs seem capable of forming a relatively normal IPL without prepatterning signals from GCs.

The disorganization of the nascent *lak* mutant IPL suggests that GCs impart order on AC neurites as they begin to project to the IPL. However, some of the errors we observed in *lak* mutants appear to result primarily from exuberant growth of ACs towards each other. In particular, the clumping of ACs and their neurites outside the IPL (Fig. 4D-G) suggested that ACs might have a tendency to attract each other. To look more directly for evidence of such cellular behavior, we made time-lapse recordings of line 243 in the *lak* background. A sample recording shows individual cells that project neurites not towards landmarks such as the ILM or the IPL, but rather towards the neurites of other ACs (see Movie 5 at

http://dev.biologists.org/supplemental). In this movie, neurites from two isolated ACs are seen approaching each other, making putative contact and forming a stable nexus of processes. Notably, each of the cells also appears to make contact with other nearby AC neurites, indicating that agglomeration errors may originate from AC-AC attraction. The *lak* mutant phenotype, therefore, reveals the existence of both GC-AC interactions and AC-AC interactions during formation of the IPL.

IPL sublamination occurs in the *lak* mutant, but is locally perturbed

We next turned our attention from IPL formation to sublamination, and asked whether this process is affected by the absence of GCs. We found that sublamination occurs late and is imperfect in *lak* mutants. By 82 hpf, the GFP plexus of wild-type retina generally shows sublamination, but it rarely does in *lak* mutants (Fig. 3; also see Fig. S3A,B at http://dev.biologists.org/supplemental). At 4 dpf, however, two distinct sublaminae have formed in mutants, similar to wild type (Fig. 5). With age (7 dpf; Fig. 5), these sublaminae were maintained, and the jagged course of the IPL appears to further straighten. However, unlike wild-type animals where ON and OFF sublaminae are parallel and continuous across the retina, sublamination is locally perturbed in *lak* mutants. One or both of the sublaminae may be absent (often replaced by a diffuse distribution of GFP^+ processes throughout the IPL), or an ectopic sublamina or non-laminar agglomerations may appear locally (Fig. 5). Multiple errors were always seen throughout the retina in every 5-7 dpf mutant eye examined (n>40). Some of these non-laminar clumps resemble structures seen in the nascent IPL of *lak* mutants (Fig. 4), suggesting that these errors occur early in development and persist to mature stages.

IPL perturbations correlate with projection errors by BCs

BCs are born a few hours later than ACs in the zebrafish retina, and their terminals arrive later in the IPL (Schmitt and Dowling, 1999) (J.N.K. and H.B., unpublished). The local disruptions in AC neuritic organization in *lak* mutants, therefore, provide an opportunity to determine whether BC axon terminals stratify normally when AC laminae are disrupted. Using an antibody against PKCβ1 (PKC) as a marker for ON BCs (Yazulla and Studholme, 2001; Connaughton, 2001; Kay et al., 2001), we assayed the BC stratification patterns of wild-type and *lak* mutants in the 220 background. In wild type, PKC-IR terminals are observed in three sublaminae of the ON (proximal) IPL. In *lak* mutants, the distribution of ON BC terminals is normal in regions where two distinct and orderly GFP^+ laminae are present (Fig. 6). However, in regions where the AC projection to the IPL is abnormal, ON BC terminals are either disorganized or, in severely perturbed regions, completely excluded from the ON IPL. BC errors were never observed in regions with normal AC stratification (n=10 *lak* retinas). These findings suggest that BCs may rely on ACs for stratification cues.

Moreover, the *lak* BC phenotype suggests that ON BCs may specifically take their cues from ON-projecting ACs. In retinal regions where the

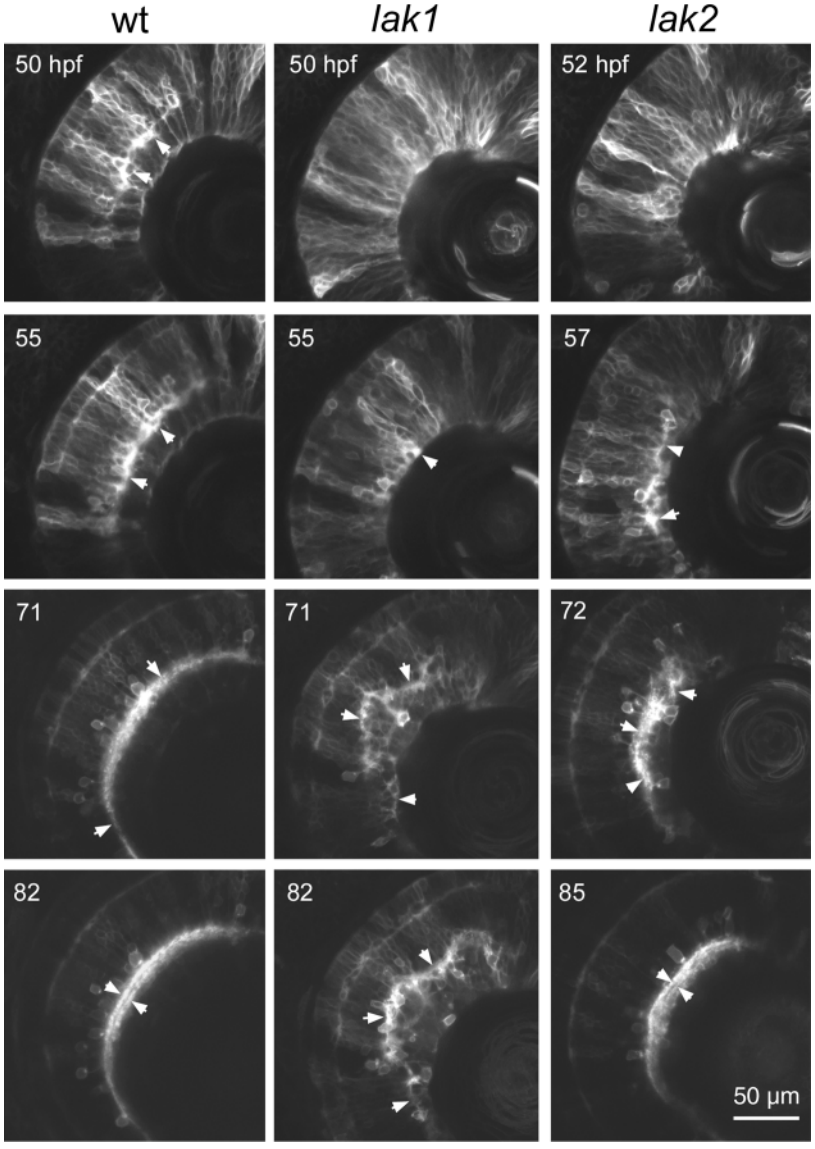

Fig. 3. In vivo comparison of IPL formation and sublamination in wild-type and *lak* mutants. Time-lapse imaging of retinas in line 220 wild-type and *lakritz* (*lak*) mutant backgrounds during IPL formation and differentiation. Both IPL formation and sublamination are delayed in the mutants. Each image is the *z*-projection of 3 μm confocal image stacks. Dorsal retina is towards the top. All three animals shown here were age-matched siblings, and were imaged concurrently. In all images, arrows indicate location of the developing IPL. Opposing arrows at 82 (wild type) and 85 (*lak*2) hpf indicate location where sublamination is apparent. Note that the IPL of *lak2* becomes more organized with time. Movies showing time-lapse recordings from additional wild-type and *lak* siblings are provided at http://dev.biologists.org/supplemental (Movie 3A,B).

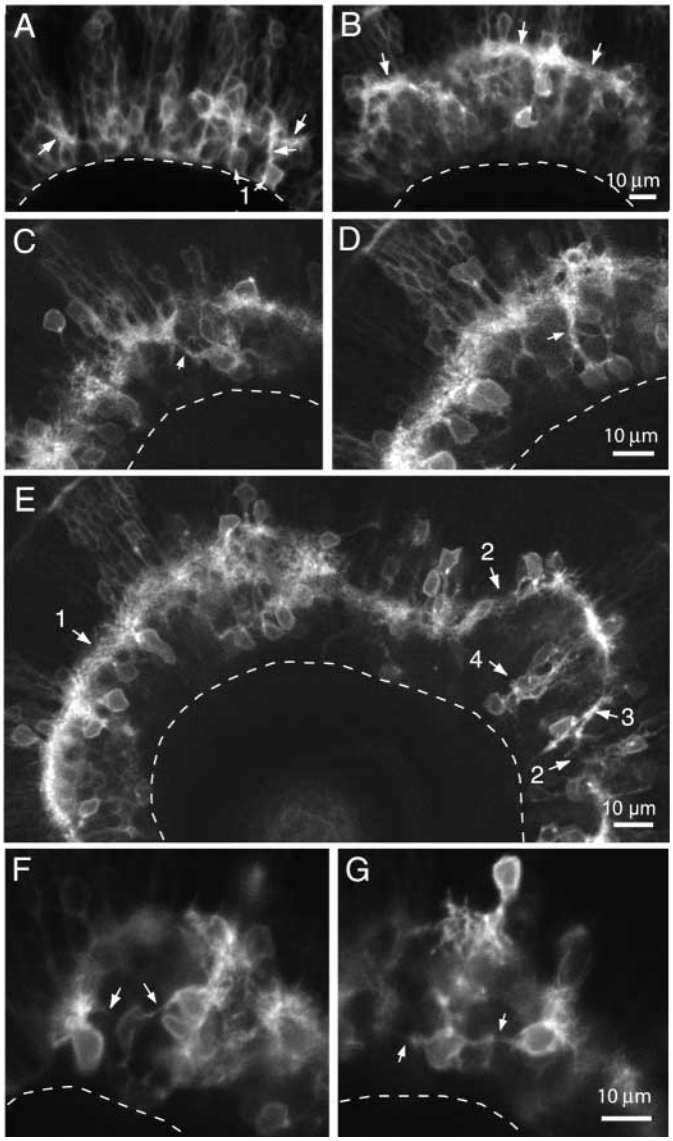

Fig. 4. AC errors during IPL formation in *lak* mutants. (A,B) Confocal images of the same region of a *lak* mutant retina at 55 hpf (A) and 71 hpf (B). GFP$^+$ AC neurites (arrows) initially accumulated near the internal limiting membrane (ILM; broken line) at various orientations, but with time, the forming IPL moved away from the ILM. Also shown in A are examples of GFP$^+$ AC bodies (1) abutting the ILM, a feature commonly observed at this early stage in the mutants, but not apparent in wild type. (C,D) A disorganized region of mutant retina at 60 (C) and 66 (D) hpf. (C) AC neurites (arrow) are oriented abnormally, growing obliquely to the ILM. (D) An ectopic bundle of AC neurites (arrow) has formed external to the IPL. Some GFP$^+$ neurites grow directly into this bundle rather than into the main GFP$^+$ plexus. (E) The *lak* retina shown in C,D at 70 hpf, demonstrating regions of relatively normal IPL location and orientation (1); abnormal regions where there are gaps in the GFP$^+$ plexus (2); neurites oriented perpendicular to the ILM (3); and GFP$^+$ AC somata agglomerating in a column (4). See Movie 4 at http://dev.biologists.org/supplemental for additional views of this retina and others of similar age. (F,G) Examples of AC neurites in an 82 hpf *lak* retina linking neighboring cells (arrows), suggesting the tendency of ACs to grow neurites toward each other despite disorganization in their cell body locations. See Movie 5, which illustrates this tendency. All panels depict line 220.

ON BCs and ACs showed severe phenotypes, the OFF AC layer was frequently observed to be relatively normal (Fig. 6). In this (Fig. 6) and several other examples, some PKC-IR BC terminals appear coincident with a fainter band of GFP$^+$ neurites ectopically located adjacent to the inner nuclear layer. It could be that the sublaminae are locally inverted here, i.e. these ectopic neurites may arise from ON ACs. If so, this raises the possibility that targeting of the ON BC terminals follows the lamination patterns of ON ACs.

The effect of the *lak* mutation on AC sublamination is cell-nonautonomous

Is the absence of GCs sufficient to explain the *lak* IPL phenotype? The *lak*/*ath5* gene is transiently expressed in most or all retinal progenitors, including those that generate the ACs (Masai et al., 2000) (J.N.K. and H.B., unpublished). It is therefore important to investigate whether the AC IPL phenotype is really due to absence of GCs, or whether the *lak* mutation affects ACs directly. To address this issue, we created *lak*/wild-type chimeras by transplanting small groups of cells from 220 carriers into non-transgenic embryos (Ho and Kane, 1990). We then fixed the chimeras at 4 dpf and inspected their retinas in whole mount for the presence of single GFP$^+$ cells (Fig. 7A-F). We found that all wild-type ACs transplanted into a wild-type retina were monostratified, either in the presumed ON or in the presumed OFF *l*ayer (n=28 cells from 12 eyes; Fig. 7A,B,G). When *lak* ACs were transplanted into wild-type retina, their morphologies were indistinguishable from wild type (n=8 cells from 4 eyes; all monostratified; Fig. 7C). However, wild-type ACs transplanted into a *lak* mutant retina occasionally (2/7 cells) had diffuse or bistratified processes (n=7 cells from two eyes; Fig. 7D). The distribution of projection errors was similar to that seen when *lak* ACs were transplanted into a *lak* host (n=7 cells from two eyes; 2/7 diffuse; Fig. 7E,F). These results suggest that the projection phenotype of an AC is determined not by its own *lak* genotype, but by that of the surrounding cells.

By sectioning chimeric animals at 7 dpf, we were able to analyze stratification of more donor-derived neurites per eye than was possible in wholemounts (Fig. 7G-J). This approach confirmed our initial findings: When wild-type or *lak* cells were transplanted into wild-type retina, we always observed GFP$^+$ neurites confined to specific sublayers of the IPL (n=8 eyes for each condition; Fig. 7G,H). However, when wild-type or *lak* cells were transplanted into *lak* retina, in every case we observed some GFP$^+$ neurites spreading diffusely throughout the IPL (n=4 eyes for each condition; Fig. 7I,J). This analysis demonstrates that the AC sublamination defects seen in the *lak* mutant retina are cell-nonautonomous and are in all likelihood caused by the absence of GCs.

Discussion

Laminated tissues provide an ideal system for studying how neurites choose specific synaptic targets in the CNS. Here, taking advantage of the optical clarity and rapid development of zebrafish embryos, we have investigated the genesis of synaptic laminae in the retina. To our knowledge, our study is the first to capture the morphogenesis of a layered synaptic structure in vivo.

The zebrafish *lak/ath5* mutant provides a unique

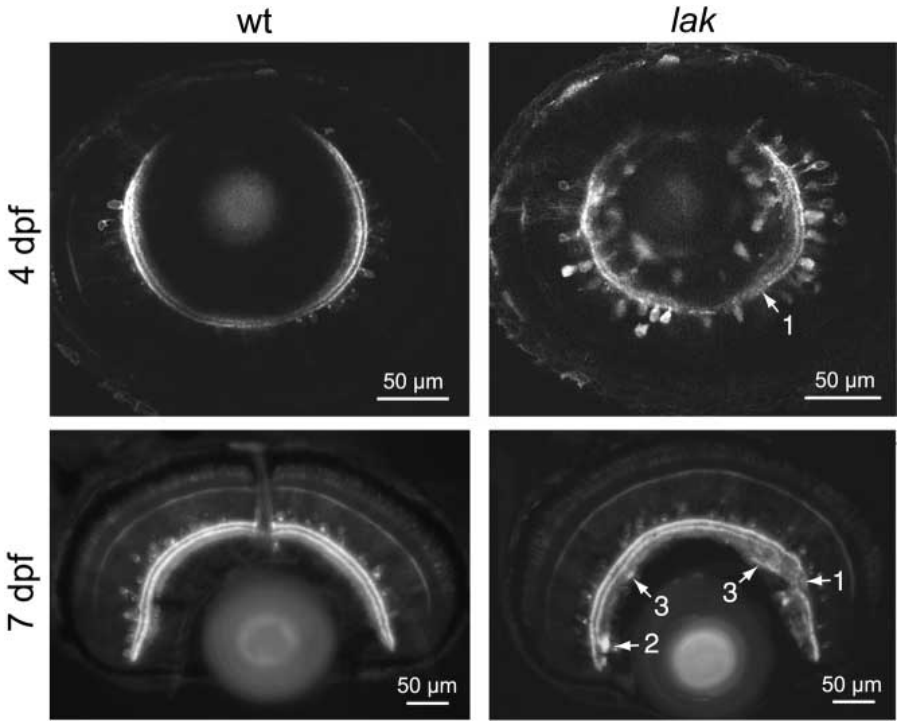

Fig. 5. Sublamination occurs in *lak* mutants but is locally perturbed. Confocal images of retinas of line 220 in wild-type and *lak* background, following IPL sublamination. At 4 and 7 days post-fertilization (dpf), two major sublaminae are observed both in wild type and in *lak* animals. However, sublamination is perturbed locally in the mutant. Sublaminae are some times absent (1), displaced relative to the adjacent regions (2) or added ectopically (3).

experimental situation in which the major postsynaptic cells of the inner retina, the GCs, are never present. Loss of *ath5* function causes a cell-fate switch that blocks GC formation and increases the number of BCs (Kay et al., 2001). However, increased BC density is unlikely to explain the AC phenotypes we report here, because these phenotypes can be observed even before BCs begin innervating the IPL (Schmitt and Dowling, 1999). The number of *Pax6-DF4:GFP*$^+$ ACs is not increased in *lak* mutants (Kay et al., 2001). Our cell transplantation experiments further convince us that the *lak* mutant can be used as a specific tool to study the effects of GC ablation on IPL development.

Time-lapse imaging of GFP-labeled AC neurites revealed the dynamics of IPL formation and ON/OFF sublamination in wild-type and mutant retinas. These studies demonstrate a previously unrecognized role for GCs in positioning and orienting AC neurites during their initial outgrowth towards the IPL. Our studies also highlight, however, the importance of ACs in IPL assembly: ACs can form the IPL on their own, and they appear to provide sublaminar targeting cues to their synaptic partners.

Migration and somal positioning of ACs are influenced by GCs

GCs are well placed to guide the migration of newborn ACs because they are the first cell type to differentiate in the vertebrate retina. In wild type, the early IPL invariably forms at the interface of GCL and the AC layer. In *lak* mutants, IPL formation begins in an ectopic location, next to the ILM. However, as ACs migrate towards the inner retina and take up

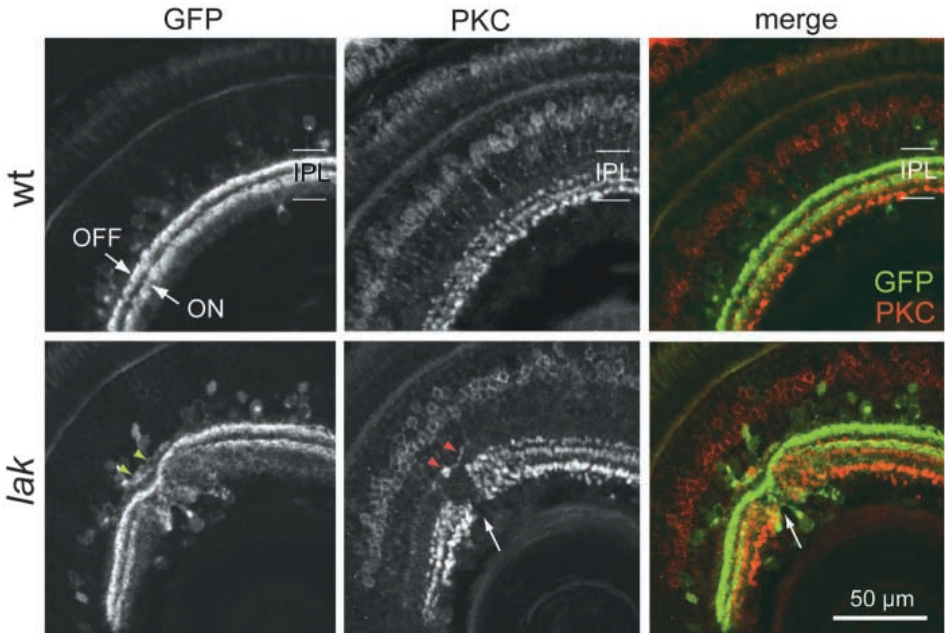

Fig. 6. BC sublaminar targeting errors follow AC errors in *lak* mutants. Confocal images of cross sections of line 220 wild-type (wt) and *lak* mutant retinas (6 dpf), immunolabeled for protein kinase C (PKC). Staining is seen in BCs with axon terminals stratifying in three sublayers of the *on* (i.e. proximal) region of the IPL. In wild type, only one of the two major GFP$^+$ AC sublaminae overlaps with the PKC-immunoreactive terminals, indicating that one is within the ON sublayer and the other is within the OFF sublayer. In *lak*, the orderly arrangement of the BC terminals is disrupted only in regions where the GFP$^+$ AC sublaminae are perturbed. Arrows indicate a local region within which the OFF GFP$^+$ lamina appears relatively normal (if contorted), and the ON lamina is either missing or displaced to the outer IPL. In this region, ON BC terminals (red arrowheads) are excluded from the ON sublamina, although a few puncta have aligned with diffuse GFP$^+$ processes in the OFF sublamina (green arrowheads).

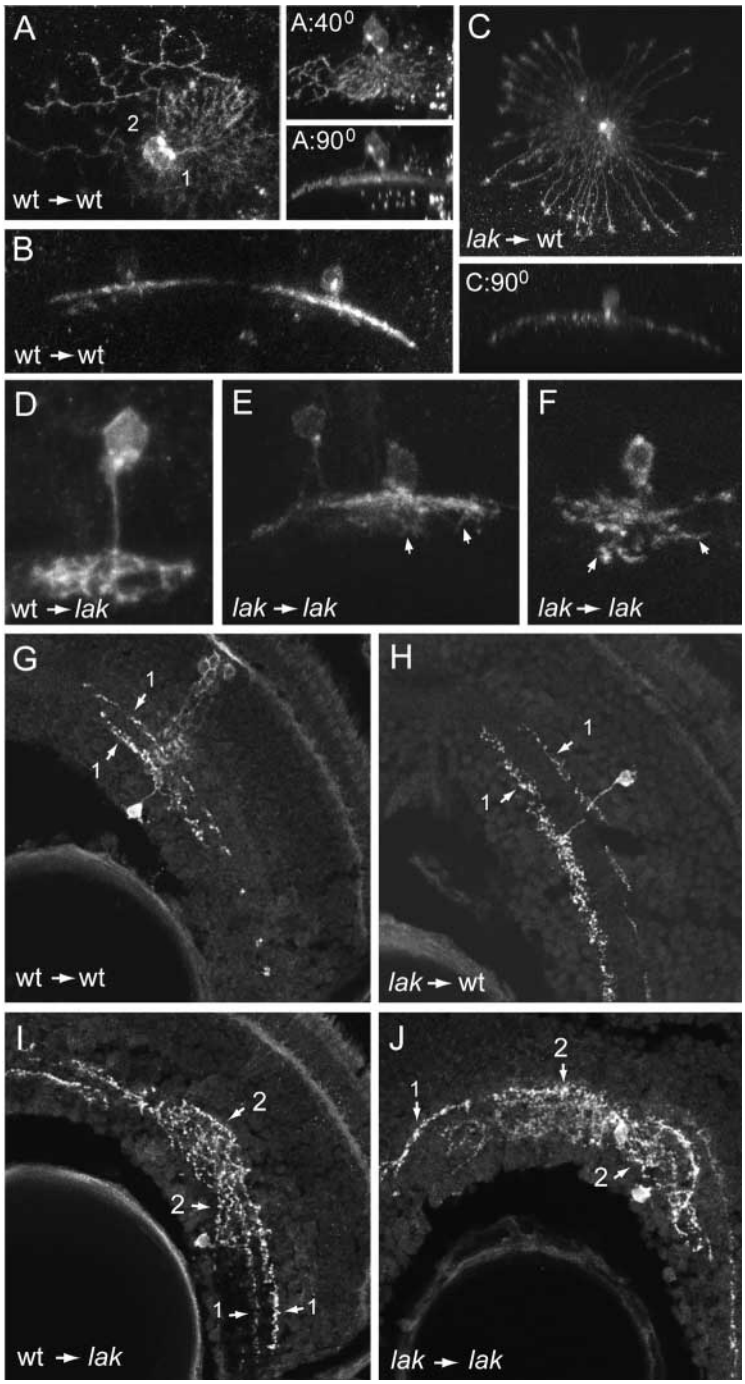

Fig. 7. The *lak* gene is not required within ACs for dendrite morphogenesis or sublaminar targeting. (A-C) Normal morphology and monostratification of line 220 GFP$^+$ ACs situated in wild-type retinas, as revealed by transplantation into non-GFP hosts. (A) Wild-type ACs in a wild-type host. Reconstructions of confocal stacks are shown *en face* and rotated 40° and 90°. Cell 1 has a symmetrical dendritic field and tightly packed processes, while Cell 2 has a larger, asymmetric dendritic field (note in the 90° rotation that the primary dendrite is already projecting to the left) and sparse, highly branched processes. Both cells are monostratified in the same IPL sublayer (see 90° rotation). (B) Two more monostratified ACs from a different wild type into wild type chimera. (C) A large-field symmetrical AC derived from a *lak* mutant develops normally in a wild-type host retina. A 90° rotation shows that its arbors are monostratified. (D-F) Projection errors of ACs situated in *lak* mutant retinas. A wild-type-derived AC in a *lak* mutant retina (D) projects diffusely into the IPL, resembling the projection errors (arrows) made by *lak* mutant ACs in mutant retinas (E,F). (G-J) Sections through chimeric retinas, cut perpendicular to the IPL. When the host retina is wild type (G,H), donor-derived GFP$^+$ AC processes are confined to specific sublayers (1), regardless of whether the donor is wild type (G) or *lak* mutant (H). Wild-type ACs in a *lak* mutant retina (I) show local perturbations of sublaminar targeting, similar to the phenotype of *lak*-into-*lak* chimeras (J). Arrow 1, normal stratification; arrow 2, disrupted stratification.

positions adjacent to the ILM, the IPL is repositioned towards the outer retina (see Fig. 8E,F for a model). These observations raise the possibility that GCs normally restrict the majority of ACs from migrating into the GCL.

AC projections to the IPL are initially guided by cues from GCs

We observed two phenotypes in the *lak* mutant, suggesting that GCs influence the early outgrowth of AC processes. First, *lak* mutants show delayed IPL formation. This is not likely to be an effect of the *lak* mutation on the timing of neurogenesis, because we showed previously that AC differentiation begins on time despite the failure of GC specification (Kay et al., 2001). Rather, this phenotype suggests that GCs may present a signal that promotes neurite outgrowth from ACs. Alternatively, it may be organization of AC neurites into a detectable plexus, not neurite outgrowth, that is delayed in the absence of GCs.

Second, the disorganization of the AC projection in the *lak* mutant suggests that signals from GCs are important for AC neurite guidance. This phenotype is not caused by the absence of Ath5 in ACs, as shown by our transplantation experiments. One possibility is that the GC-derived signals act at a distance to orient AC growth towards the nascent IPL (Fig. 8D); another possibility is that contact between AC and GC neuritic processes stabilizes appropriately directed neurites while destabilizing misguided ones.

The severe IPL phenotype seen in *lak* mutants contrasts with the relatively mild effects of GC ablation by optic nerve transection (Günhan-Agar et al., 2000; Williams et al., 2001). In the latter studies, GCs form but are experimentally killed in newborn rats or ferrets. We suggest that the different outcomes of these experiments demonstrate that even transient presence of GCs can pattern the IPL.

ACs can form the IPL alone

GC-derived cues are not the only signals capable of guiding AC neurites, given that many ACs in *lak* mutants either project normally to the IPL or correct their early errors It is unlikely that BC terminals provide AC guidance signals, as they have yet to innervate the IPL during the time when ACs are doing so (Schmitt and Dowling, 1999) (J.N.K., A.M. and H.B., unpublished). Similarly, Müller glia differentiate too late to

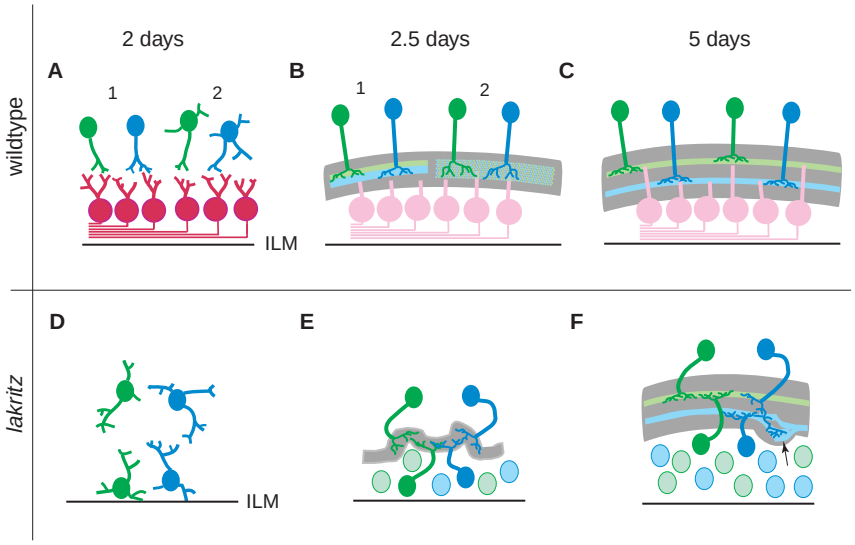

Fig. 8. Model of IPL formation and sublamination in wild-type and *lak* mutants. (A-C) IPL formation in wild-type retina. At 2 dpf (A), ACs (green, blue) start to grow neurites. GCs and/or their dendrites (red), which have already grown out to form a proto-IPL, provide a signal that either orients ACs and their processes towards the nascent IPL (model 1, left), or else stabilizes IPL-oriented processes (model 2, right). At 2.5 dpf (B), ON (blue) and OFF (green) ACs have ramified their dendrites within the IPL (gray shaded area), but separate sublayers are not yet distinguishable. ON and OFF IPL domains (light blue and green shading) may already be distinct, but so close together within the developing IPL that they look like a single diffuse layer (model 1, represented by the two left-hand cells in B). Alternatively, ON and OFF strata may not be separate yet at this stage, in which case ACs would project diffusely throughout the extent of the IPL (model 2; right-hand cells of B). By 5 dpf (C), distinct ON and OFF sublayers are clearly evident. GCs are shown in pink; their dendrites are not fully depicted in B or C. (D-F) IPL formation in the absence of GCs. In *lak* mutants at 2 dpf (D), ACs lack the orienting signal from GCs and grow neurites in random directions, or towards each other. Their cell bodies are often ectopically positioned adjacent to the ILM, which causes the early IPL to form there as well. By 2.5 dpf (E), the tendency of AC neurites to grow towards each other has led to formation of an IPL. Because of the initial disorganization of AC somata and neurites, however, the nascent IPL is uneven. AC somata continue to accumulate between the IPL and the ILM, forming a layer of 'misplaced' ACs. By 5 dpf (F), much of the unevenness has dissipated and IPL sublayers have formed, indicating that there are cues available to ACs that allow correction of early errors. One such mechanism may be homotypic attraction between ACs. However, these cues are not sufficient to allow correction of every error, leading to local perturbations of IPL sublamination (arrow).

guide the initial projection of ACs (Peterson et al., 2001). As the *lak* mutant IPL consists predominantly of ACs at these early time points, ACs do not seem to require interactions with other IPL constituents in order to form an IPL-like plexus.

How do AC neurites form an IPL in *lak* mutants? It is possible that interactions with neuroepithelial cells might guide AC projections. However, our observations suggest another possibility, that AC-AC attraction may be sufficient for IPL formation. Many of the errors made by GFP^+ ACs in *lak* mutants are most easily explained if we postulate that ACs can attract each other: The tendency of AC somata and neurites to clump, and the observation of newly differentiating adjacent ACs extending neurites directly towards each other, rather than towards the IPL, are particularly suggestive of attractive behavior. Our imaging study cannot provide definitive proof of AC-AC attraction, but we hypothesize based on our findings that such attraction does indeed exist, and we suggest that this attraction is probably the mechanism that explains the eventual assembly of a relatively normal IPL in *lak* mutants. Through AC-AC attraction, early errors could be corrected and later-arriving AC neurites could be correctly guided to the IPL (Fig. 8).

Together, our studies lead to a model of IPL formation in which ACs interact with GCs, and with each other, during assembly of the wild type IPL (Fig. 8). The interaction with GCs may be most important for positioning somata and orienting early outgrowth, whereas the attractive influence of other ACs and their neurites may stimulate AC innervation of the IPL.

ACs may drive IPL sublamination

We used line 220 to investigate how sublamination arises during development. We found that the nascent IPL is not obviously stratified (Fig. 2C) but over a period of about 10 hours, distinct ON and OFF sublaminae form. Sublamination sweeps across the retina in approximately the same spatiotemporal pattern that characterizes the wave of AC neurogenesis, as has recently been suggested from static images of the chick retina (Drenhaus et al., 2003). This behavior suggests that sublamination may occur at a fixed time after cell specification. Alternatively, there may be a progressive mechanism for sublamination that propagates through the IPL in a wave-like manner. In either case, our recordings have revealed that the IPL undergoes significant morphogenesis between 60 and 70 hpf that results in the formation of distinct sublayers.

We then asked if sublamination involves interactions between ACs and their major postsynaptic target, the GCs. Our results demonstrate that GCs are dispensable for sublamination of AC and BC projections, as previously suggested by experiments in which GCs were removed postnatally in mammals (Günhan-Agar et al., 2000; Williams et al., 2001). Might other retinal cell types provide signals for AC/BC sublaminar targeting? A mouse mutant lacking BCs shows normal AC sublamination (Green et al., 2003); it therefore seems unlikely that ACs receive sublaminar cues from BCs. Müller glia, which first differentiate around 60-70 hpf (Peterson et al., 2001), are another potential source of sublamination cues. Our findings in *lak* mutants suggest that AC neurites carry at least some targeting cues for their synaptic partners: In areas of the mutant retina where sublaminar information from ACs is degraded or lost, ON BCs fail to target correctly. Recent molecular studies suggest that these AC-derived cues could take the form of homophilic cell adhesion molecules, such as Ig-superfamily molecules or cadherins (Yamagata et al., 2002; Masai et al., 2003).

Despite the fact that GCs are not essential for sublamination, the IPL is not completely normal in *lak* mutants – we found that sublamination is globally delayed, and that it fails altogether in local retinal patches. Such findings are consistent with the possibility that GCs provide one of several signals that influence sublamination. However, we think it is more likely that the presence of GCs is permissive: GCs may provide a scaffold that organizes the early IPL, setting the stage for a GC-independent sublamination process. According to this model, the initially-disorganized IPL that forms in the absence of GCs needs time to 'recover' (self-correct by AC-AC interactions) before sublamination can start. That recovery does occur is shown by our time-lapse images – the unevenness and disorganization of the *lak* mutant IPL clearly improves with time. The retinal patches where sublamination fails may correspond to places where the early disorganization does not recover sufficiently to allow sublamination – for example, in places where an ectopic aggregate of AC processes has formed (see model in Fig. 8).

Targeting without a major target

Our finding that the presence of a major class of postsynaptic neurons is dispensable for the proper arrangement of presynaptic terminals is not without precedent. In the *Drosophila* optic lobe and the mouse entorhinal-hippocampal projection, afferents depend on a transient intermediate target rather than the eventual postsynaptic neuron for correct sublaminar targeting (Huang and Kunes, 1996; Poeck et al., 2001; Suh et al., 2002; Del Rio et al., 1997). In contrast to these earlier studies, we show that ablation of GCs disrupts the initial targeting of ACs, but that most of these errors are later corrected. Our study therefore indicates that targeting cues are provided both by postsynaptic partners and by presynaptic neighbors. The picture that emerges is that of a delicately orchestrated interplay of intrinsic programs and cell-cell interactions that act together (sometimes in overlapping fashion) to bring axons into register in the target zone.

This work was supported by an NSF predoctoral fellowship (J.N.K.), by a Boehringer Ingelheim fellowship (T.R.), by a NIH NRSA fellowship (J.S.M.), by the NEI (R.O.L.W. and H.B.) and by a David and Lucile Packard Fellowship (H.B.).

References

Bodnarenko, S. R. and Chalupa, L. M. (1993). Stratification of ON and OFF ganglion cell dendrites depends on glutamate-mediated afferent activity in the developing retina. *Nature* **364**, 144-146.

Bodnarenko, S. R., Jeyarasasingam, G. and Chalupa, L. M. (1995). Development and regulation of dendritic stratification in retinal ganglion cells by glutamate-mediated afferent activity. *J. Neurosci.* **15**, 7037-7045.

Brown, N. L., Patel, S., Brzezinski, J. and Glaser, T. (2001). Math5 is required for retinal ganglion cell and optic nerve formation. *Development* **128**, 2497-2508.

Connaughton, V. P. (2001). Organization of ON- and OFF-pathways in the zebrafish retina: neurotransmitter localization, electrophysiological responses of bipolar cells, and patterns of axon terminal stratification. *Prog. Brain Res.* **131**, 161-176.

Constantine-Paton, M., Cline, H. T. and Debski, E. (1990). Patterned activity, synaptic convergence, and the NMDA receptor in developing visual pathways. *Annu. Rev. Neurosci.* **13**, 129-154.

Del Rio, J. A., Heimrich, B., Borrell, V., Forster, E., Drakew, A., Alcantara, S., Nakajima, K., Miyata, T., Ogawa, M., Mikoshiba, K. et al. (1997). A role for Cajal-Retzius cells and reelin in the development of hippocampal connections. *Nature* **385**, 70-74.

Drenhaus, U., Morino, P. and Veh, R. W. (2003). On the development of the stratification of the inner plexiform layer in the chick retina. *J. Comp. Neurol.* **460**, 1-12.

Easter, S. S., Jr and Nicola, G. N. (1996). The development of vision in the zebrafish (Danio rerio). *Dev. Biol.* **180**, 646-663.

Famiglietti, E. V., Jr and Kolb, H. (1976). Structural basis for ON-and OFF-center responses in retinal ganglion cells. *Science* **194**, 193-195.

Green, E. S., Stubbs, J. L. and Levine, E. M. (2003). Genetic rescue of cell number in a mouse model of microphthalmia: interactions between Chx10 and G1-phase cell cycle regulators. *Development* **130**, 539-552.

Günhan-Agar, E., Kahn, D. and Chalupa, L. M. (2000). Segregation of on and off bipolar cell axonal arbors in the absence of retinal ganglion cells. *J. Neurosci*. **20**, 306-314.

Higashijima, S., Okamoto, H., Ueno, N., Hotta, Y. and Eguchi, G. (1997). High-frequency generation of transgenic zebrafish which reliably express GFP in whole muscles or the whole body by using promoters of zebrafish origin. *Dev. Biol.* **192**, 289-299.

Hitchcock, P. F., Macdonald, R. E., VanDeRyt, J. T. and Wilson, S. W. (1996). Antibodies against Pax6 immunostain amacrine and ganglion cells and neuronal progenitors, but not rod precursors, in the normal and regenerating retina of the goldfish. *J. Neurobiol.* **29**, 399-413.

Ho, R. K. and Kane, D. A. (1990). Cell-autonomous action of zebrafish spt-1 mutation in specific mesodermal precursors. *Nature* **348**, 728-730.

Hu, M. and Easter, S. S. (1999). Retinal neurogenesis: the formation of the initial central patch of postmitotic cells. *Dev. Biol.* **207**, 309-321.

Huang, Z. and Kunes, S. (1996). Hedgehog, transmitted along retinal axons, triggers neurogenesis in the developing visual centers of the Drosophila brain. *Cell* **86**, 411-422.

Johnson, A. D. and Krieg, P. A. (1994). pXeX, a vector for efficient expression of cloned sequences in Xenopus embryos. *Gene* **147**, 223-226.

Kammandel, B., Chowdhury, K., Stoykova, A., Aparicio, S., Brenner, S. and Gruss, P. (1999). Distinct cis-essential modules direct the time-space pattern of the Pax6 gene activity. *Dev. Biol*. **205**, 79-97.

Katz, L. C. and Shatz, C. J. (1996). Synaptic activity and the construction of cortical circuits. *Science* **274**, 1133-1138.

Katz, L. C. and Crowley, J. C. (2002). Development of cortical circuits: lessons from ocular dominance columns. *Nat. Rev. Neurosci.* **3**, 34-42.

Kay, J. N., Finger-Baier, K. C., Roeser, T., Staub, W. and Baier, H. (2001). Retinal ganglion cell genesis requires *lakritz*, a zebrafish *atonal* homolog. *Neuron* **30**, 725-736.

Kelsh, R. N., Brand, M., Jiang, Y. J., Heisenberg, C. P., Lin, S., Haffter, P., Odenthal, J., Mullins, M. C., van Eeden, F. J., Furutani-Seiki, M. et al. (1996). Zebrafish pigmentation mutations and the processes of neural crest development. *Development* **123**, 369-389.

Livesey, F. J. and Cepko, C. L. (2001). Vertebrate neural cell-fate determination: lessons from the retina. *Nat. Rev. Neurosci*. **2**, 109-118.

Marquardt, T., Ashery-Padan, R., Andrejewski, N., Scardigli, R., Guillemot, F. and Gruss, P. (2001). Pax6 is required for the multipotent state of retinal progenitor cells. *Cell* **105**, 43-55.

Masai, I., Stemple, D. L., Okamoto, H. and Wilson, S. W. (2000). Midline signals regulate retinal neurogenesis in zebrafish. *Neuron* **27**, 251-263.

Masai, I., Lele, Z., Yamaguchi, M., Komori, A., Nakata, A., Nishiwaki, Y., Wada, H., Tanaka, H., Nojima, Y., Hammerschmidt, M. et al. (2003). N-cadherin mediates retinal lamination, maintenance of forebrain compartments and patterning of retinal neurites. *Development* **130**, 2479-2494.

Maslim, J. and Stone, J. (1988). Time course of stratification of the dendritic fields of ganglion cells in the retina of the cat. *Dev. Brain Res.* **44**, 87-93.

Miles, C., Elgar, G., Coles, E., Kleinjan, D. J., van Heyningen, V. and Hastie, N. (1998). Complete sequencing of the Fugu WAGR region from WT1 to PAX6: dramatic compaction and conservation of synteny with human chromosome 11p13. *Proc. Natl. Acad. Sci. USA* **95**, 13068-13072.

Peterson, R. E., Fadool, J. M., McClintock, J. and Linser, P. J. (2001). Muller cell differentiation in the zebrafish neural retina: evidence of distinct early and late stages in cell maturation. *J. Comp. Neurol.* **429**, 530-540.

Plaza, S., Dozier, C., Langlois, M. C. and Saule, S. (1995). Identification and characterization of a neuroretina-specific enhancer element in the quail Pax-6 (Pax-QNR) gene. *Mol. Cell. Biol.* **15**, 892-903.

Poeck, B., Fischer, S., Gunning, D., Zipursky, S. L. and Salecker, I. (2001). Glial cells mediate target layer selection of retinal axons in the developing visual system of Drosophila. *Neuron* **29**, 99-113.

Pow, D. V., Crook, D. K. and Wong, R. O. (1994). Early appearance and

transient expression of putative amino acid neurotransmitters and related molecules in the developing rabbit retina: an immunocytochemical study. *Vis. Neurosci.* **11**, 1115-1134.

Reese, B. E., Raven, M. A., Giannotti, K. A. and Johnson, P. T. (2001). Development of cholinergic amacrine cell stratification in the ferret retina and the effects of early excitotoxic ablation. *Vis. Neurosci.* **18**, 559-570.

Roska, B. and Werblin, F. (2001). Vertical interactions across ten parallel, stacked representations in the mammalian retina. *Nature* **410**, 583-587.

Sanes, J. R. and Yamagata, M. (1999). Formation of lamina-specific synaptic connections. *Curr. Opin. Neurobiol.* **9**, 79-87.

Schmitt, E. A. and Dowling, J. E. (1999). Early retinal development in the zebrafish, Danio rerio: light and electron microscopic analyses. *J. Comp. Neurol.* **404**, 515-536.

Siemering, K. R., Golbik, R., Sever, R. and Haseloff, J. (1996). Mutations that suppress the thermosensitivity of green fluorescent protein. *Curr. Biol.* **6**, 1653-1663.

Skene, J. H. and Virag, I. (1989). Posttranslational membrane attachment and dynamic fatty acylation of a neuronal growth cone protein, GAP-43. *J. Cell Biol.* **108**, 613-624.

Stacy, R. C. and Wong, R. O. L. (2003). Developmental relationship between cholinergic amacrine cell processes and ganglion cell dendrites of the mouse retina. *J. Comp. Neurol.* **456**, 154-166.

Stuart, G. W., McMurray, J. V. and Westerfield, M. (1988). Replication, integration and stable germ-line transmission of foreign sequences injected into early zebrafish embryos. *Development* **103**, 403-412.

Suh, G. S., Poeck, B., Chouard, T., Oron, E., Segal, D., Chamovitz, D. A. and Zipursky, S. L. (2002). Drosophila JAB1/CSN5 acts in photoreceptor cells to induce glial cells. *Neuron* **33**, 35-46.

Wang, S. W., Kim, B. S., Ding, K., Wang, H., Sun, D., Johnson, R. L., Klein, W. H. and Gan, L. (2001). Requirement for math5 in the development of retinal ganglion cells. *Genes Dev.* **15**, 24-29.

Wässle, H. and Boycott, B. B. (1991). Functional architecture of the mammalian retina. *Physiol. Rev.* **71**, 447-480.

Williams, R. R., Cusato, K., Raven, M. A. and Reese, B. E. (2001). Organization of the inner retina following early elimination of the retinal ganglion cell population: effects on cell numbers and stratification patterns. *Vis. Neurosci.* **18**, 233-244.

Wong, R. O. L. and Lichtman, J. W. (2002). Synapse elimination. In *Fundamental Neuroscience* (ed. M. J. Zigmond, F. E. Bloom, S. C. Landis, J. L. Roberts and L. R. Squire), pp. 533-554. San Diego, CA: Academic Press.

Yamagata, M., Weiner, J. A. and Sanes, J. R. (2002). Sidekicks: synaptic adhesion molecules that promote lamina-specific connectivity in the retina. *Cell* **110**, 649-660.

Yazulla, S. and Studholme, K. M. (2001). Neurochemical anatomy of the zebrafish retina as determined by immunocytochemistry. *J. Neurocytol.* **30**, 551-592.

Zhang, L. I. and Poo, M. M. (2001). Electrical activity and development of neural circuits. *Nat. Neurosci. Suppl.* 1207-1214.

Zuber, M. X., Strittmatter, S. M. and Fishman, M. C. (1989). A membrane-targeting signal in the amino terminus of the neuronal protein GAP-43. *Nature* **341**, 345-348.